

Quantum Data Bus in Dipolar Coupled Nuclear Spin Qubits

Jingfu Zhang*,¹ Michael Ditty,¹ Daniel Burgarth†,² Colm A. Ryan,¹ C. M. Chandrashekar,^{1,3}
 Martin Laforest,¹ Osama Moussa,¹ Jonathan Baugh,¹ and Raymond Laflamme‡^{1,3}

¹*Institute for Quantum Computing and Department of Physics,
 University of Waterloo, Waterloo, Ontario, Canada N2L 3G1*

²*IMS and QOLS, Imperial College, London SW7 2BK, UK*

³*Perimeter Institute for Theoretical Physics, Waterloo, Ontario, N2J 2W9, Canada*

(Dated: February 6, 2020)

We implement an iterative quantum state transfer exploiting the natural dipolar couplings in a spin chain of a liquid crystal NMR system. During each iteration a finite part of the amplitude of the state is transferred and by applying an external operation on only the last two spins the transferred state is made to accumulate on the spin at the end point. The transfer becomes perfect asymptotically through increasing the number of iterations. We also implement the inverted unitary evolution which can transfer the state to any other position of the chain and generate entanglement in the chain, acting as a full quantum data bus.

PACS numbers: 03.67.Lx

In quantum computation and quantum communication the transfer of an arbitrary quantum state from one qubit to another is a basic but important element. The most obvious method to implement quantum state transfer (QST) on an array of qubits is based on a sequence of SWAP operations. This protocol requires a large number of controls for interqubit interactions. Each control can introduce errors during experimental implementation. This makes the direct implementation of such gates on a large spin system challenging. Also, addressing single qubits in large size solid NMR systems is usually challenging.

To overcome this problem, schemes based on "always on" spin systems were proposed [1, 2]. The state can be transferred with unit fidelity in engineered spin chains or networks [3, 4]. However, such chains and networks are hard to implement. In other schemes based on spin chains with Heisenberg interactions [1, 5] or with a double-quantum Hamiltonian [6], the fidelity of the QST cannot approach unity in scalable systems.

The above limitations can be relaxed significantly by applying gate operations to receive and store the transferred state [7, 8]. The gates are only applied to two spins at one end of a spin chain. In this Letter, we experimentally implement the QST in a liquid crystal NMR system based on this scheme. Opposed to previous experimental implementations [8], the dipolar couplings exist naturally in the system and are directly exploited for the QST. The transfer with high fidelity is achieved in an iterative manner. Each iteration transfers a finite part of the input amplitude to the target spin at the end of the chain. The fidelity of the transfer asymptotically approaches unity by increasing the number of iterations. We also exper-

imentally demonstrate the time-inverted version of [7]. Through this, a full *quantum data bus* is implemented, where arbitrary unknown quantum states can be steered to an *any* position of the chain. This is also useful for the selective excitation of one spin, which is addressed by the two-spin gates, rather than by its individual properties, e.g. chemical shift in NMR. As opposed to previous schemes [9], global control is not required. Surprisingly the reversal operation can also be used to *entangle* any pair of spins in the chain by operation at its end only. We demonstrate this by entangling the end qubits of the chain.

The QST and its reversal operations mean that the chain is really used as a wire with an input, an output, and no gates in the middle, and only the many-body Hamiltonian of the chain is responsible for the transport. The required number of gates to achieve a good fidelity of transfer scales roughly linearly with the system size [7]. Hence our method is scalable and suitable for large-size systems, such as solid or liquid crystal NMR systems, where the differences of the chemical shifts are too small to address the spins.

Our first purpose is to transfer state $\alpha|0\rangle + \beta|1\rangle$ from spins j to N in a N -spin chain. The Hamiltonian for spins 1 to $N - 1$ is represented as

$$H = \frac{1}{2}\pi \sum_{j,k=1;k>j}^{N-1} D_{jk}(2\sigma_z^j\sigma_z^k - \sigma_x^j\sigma_x^k - \sigma_y^j\sigma_y^k), \quad (1)$$

where D_{jk} denote the dipolar coupling strengths and $\sigma_{x/y/z}^j$ denote the Pauli matrices with j indicating the affected spin. Noting that H preserves the total number of excited spins [1, 3], we have $U_\tau|\mathbf{0}\rangle = e^{i\theta}|\mathbf{0}\rangle$ and

$$U_\tau|\mathbf{j}\rangle = \sum_{k=1}^{N-1} A_k|\mathbf{k}\rangle. \quad (2)$$

Here $U_\tau = e^{-i\tau H}$ and $e^{i\theta}$ is the $(1, 1)$ matrix element of

*Corresponding author: zhangjfu2000@yahoo.com

†Corresponding author d.burgarth@imperial.ac.uk

‡Corresponding author: laflamme@iqc.ca

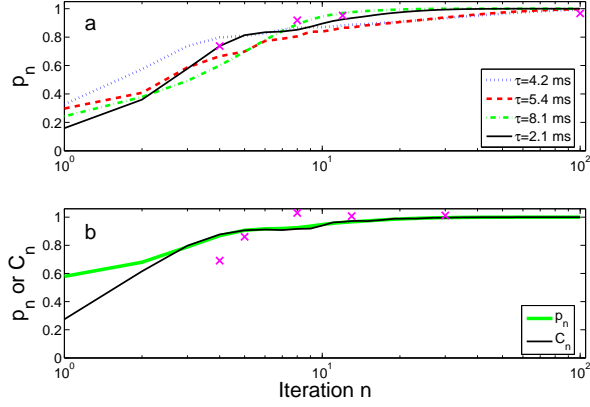


FIG. 1: (Color online) The numerical simulation (curves) and experimental results (data marked by "x") for the probability p_n of the QST as a function of iterations in the four spin system used in experiments (see text for dipolar couplings) for transferring a state from spins 1 to 4 (a) and entangling the two spins (b). In experiments τ is chosen as 2.1 ms. In figure (b) p_n can be approximated as the observable coherence C_n [see Eq. (10)] when $n > 2$.

U_τ . The state $|\mathbf{0}\rangle$ denotes all spins pointing up, and $|\mathbf{j}\rangle$ denotes all spins up except the spin j pointing down.

The main operation is the two-spin gate applied only on spins $N-1$ and N , and in iteration n the gate is denoted as

$$W(c_n, d_n) = I_{1,2,\dots,N-2} \otimes \begin{pmatrix} 1 & 0 & 0 & 0 \\ 0 & d_n^* & c_n^* & 0 \\ 0 & -c_n & d_n & 0 \\ 0 & 0 & 0 & 1 \end{pmatrix}_{N-1,N} \quad (3)$$

where $I_{1,2,\dots,N-2}$ denotes the unit operator for spins 1 to $N-2$. One can obtain $W(c_n, d_n)(c_n|\mathbf{N}-1\rangle + d_n|\mathbf{N}\rangle) = |\mathbf{N}\rangle$.

The N spin system is initialized into the input state $\alpha|\mathbf{0}\rangle + \beta|\mathbf{j}\rangle$ by setting spin j in the system to state $\alpha|0\rangle + \beta|1\rangle$. Here j is the location of the sender (receiver) of the QST for the (inverse) protocol, which is on some arbitrary spin of the quantum data bus. It is sufficient to only discuss the transfer of $|\psi_0\rangle = |\mathbf{j}\rangle$ because U_τ only introduces a phase before $|\mathbf{0}\rangle$ and W does not change $|\mathbf{0}\rangle$. Iteration n is represented as

$$Q_{j,n} = [I_{1,2,\dots,N-2} \otimes W(c_n, d_n)][U_\tau \otimes I_N]. \quad (4)$$

Using Eqs. (2-4), one can obtain the state in an iterative manner

$$|\psi_{n+1}\rangle = Q_{j,n+1}|\psi_n\rangle = \sum_{k=1}^N A_{k,n+1}|\mathbf{k}\rangle \quad (5)$$

Here $A_{N-1,n+1} = 0$, $A_{N,n+1} = \sqrt{p_{n+1}}$ where $p_0 = 0$ and $p_{n+1} = p_n + |\langle \mathbf{N}-1 | U_\tau \otimes I_N | \psi_n \rangle|^2$, $d_{n+1} = e^{i\theta} \sqrt{p_n} / \sqrt{p_{n+1}}$ and $c_{n+1} = \langle \mathbf{N}-1 | U_\tau \otimes I_N | \psi_n \rangle / \sqrt{p_{n+1}}$.

In strict nearest-neighbour chains it can be shown [7] that p_n converges to unity by increasing the number of iterations. In the present case we have also non-nearest neighbour interactions, but numerical results show p_n still approaches unity, with a convergence speed which depends on the evolution time τ [see Fig. 1 (a)]. Hence the process of QST after a large number of iterations can be presented as

$$T_{j,n}(\alpha|\mathbf{0}\rangle + \beta|\mathbf{j}\rangle) \rightarrow \alpha e^{in\theta}|\mathbf{0}\rangle + \beta|\mathbf{N}\rangle, \quad (6)$$

i.e., spin N lies in $\alpha e^{in\theta}|0\rangle + \beta|1\rangle$, where

$$T_{j,n} = Q_{j,n} \dots Q_{j,2} Q_{j,1}. \quad (7)$$

We can exploit the inversion of $T_{j,n}$ to implement the QST from spin N to spin j , i.e., without applying the external operation directly on the spin j to evolve it into state $\alpha|0\rangle + \beta|1\rangle$. Hence the spin chain functions as a *quantum data bus*, which can transfer arbitrary unknown states to any qubit. This method also allows to create a selective excitation that does not require its individual parameters, e.g. chemical shift in NMR, to address spin j . Hence it is suitable for the systems where the individual parameters of spins cannot be used for addressing. The external operations are only applied to spins $N-1$ and N . From Eqs. (5) and (7) one finds

$$p_n = |\langle \psi_0 | T_{j,n}^{-1} | \mathbf{N} \rangle|^2, \quad (8)$$

i.e., p_n is the fidelity for generating $|\psi_0\rangle$ by applying $T_{j,n}^{-1}$ to $|\mathbf{N}\rangle$. By modifying the input state one can obtain $T_{j,n}^{-1}(\alpha e^{in\theta}|\mathbf{0}\rangle + \beta|\mathbf{N}\rangle) \rightarrow \alpha|\mathbf{0}\rangle + \beta|\mathbf{j}\rangle$ [10].

The method of inverse QST furthermore can be used to entangle arbitrary spins j, k indirectly by acting at spins $N-1$ and N only. This can be done by designing a pulse analogously to Eq. (4) through setting $|\psi_0\rangle = |\psi_{jk}\rangle = (|\mathbf{j}\rangle + |\mathbf{k}\rangle) / \sqrt{2}$ and replacing p_0 as $p_0 = |\langle \mathbf{N} | \psi_{jk} \rangle|^2$. The process is represented as

$$T_{j,k,n}|\psi_{jk}\rangle \rightarrow |\mathbf{N}\rangle, \quad (9)$$

and applying $T_{j,k,n}^{-1}$ on $|\mathbf{N}\rangle$. The required pulse sequence is very similar to the inverse QST. The fidelity for generating $|\psi_{jk}\rangle$ is also represented by Eq. (8) through replacing $T_{j,n}^{-1}$ by $T_{j,k,n}^{-1}$. The numerical simulation for p_n is illustrated as Figure 1 (b).

We use the four protons in ortho-chlorobromobenzene (C_6H_4ClBr) dissolved in the liquid crystal solvent ZLI-1132 as four qubits to implement the experiments. Using Cory48 [11] and 1-D MREV-8 pulse sequences and referring to the spectra of molecules with similar structures [12], we obtain the Hamiltonian of the spin system by fitting the spectra. The chemical shifts are measured to be 393.6, 98.4, 229.3, 376.7 with respect to the transmitter frequency, dipolar couplings are $D_{12} = -1233.7$, $D_{13} = -149.4$, $D_{14} = -93.2$, $D_{23} = -716.0$, $D_{24} = -236.6$, $D_{34} = -1677.5$ Hz, and the effective transverse relaxation times (T_2^*) for the four protons are 91, 87, 88 and 82 ms.

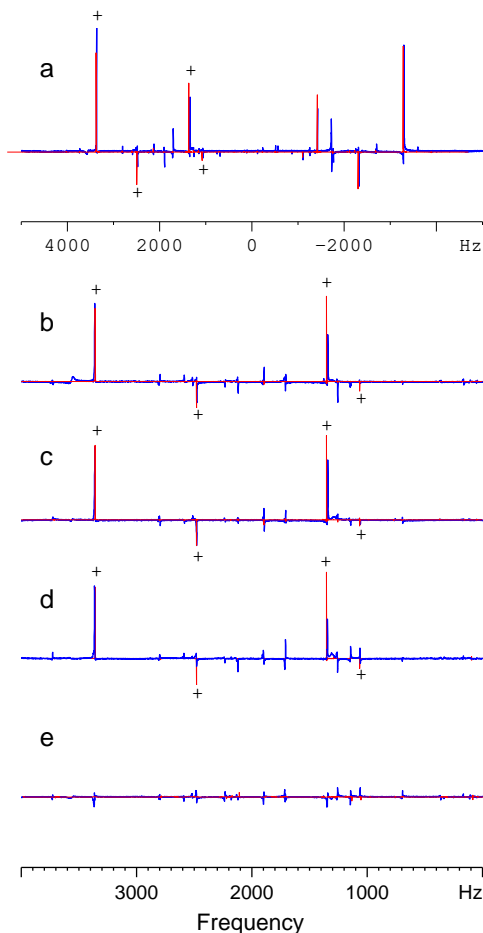


FIG. 2: (Color online) NMR spectra for implementing the QST from spins 1 to 4 in experiment (blue thick) and simulation (red thin). The plot's vertical axes have arbitrary units, but have the same scale. (a) Spectrum obtained by applying $e^{-i\pi\sigma_y^4/4}$ to ρ_{ini} . The peaks marked by "+" indicate the single quantum transitions with which we are concerned. (b-e) Spectra for the QST after 100 iterations when the input states are chosen as $\sigma_x|000\rangle\langle 000|$, $\sigma_y|000\rangle\langle 000|$, $\sigma_z|000\rangle\langle 000|$, and $I|000\rangle\langle 000|$, respectively, where the readout operation $e^{i\pi\sigma_y^4/4}$ is applied to obtain observable signals in (d) and (e).

Our experiments start with the deviation density matrix $\rho_{ini} = |0000\rangle\langle 0000| - |1111\rangle\langle 1111|$, which can be prepared by the double quantum coherence Hamiltonian [13] $H_d = \frac{1}{2}\pi \sum_{k=2, j < k}^4 D_{jk}^d (\sigma_x^j \sigma_x^k - \sigma_y^j \sigma_y^k)$ from the thermal equilibrium state $\rho_{th} = \sum_{i=1}^4 \sigma_z^i$, using a molecule with C_{2v} symmetry [14]. Alternatively, we generate the effective H_d with such symmetry in our molecule through a GRadiant Ascent Pulse Engineering pulse [15]. Using temporal averaging, we prepare ρ_{ini} by summing the four states $U_d \rho_{th} U_d^\dagger$, $U_d^\dagger \rho_{th} U_d$, ρ_{th} , ρ_{th} , where $U_d = e^{-it_d H_d}$ by choosing $t_d = 8.00/D_{12}^d$ [14]. In the numerical simulation of ρ_{ini} the diagonal elements except (1,1) and (16,16) are almost zero [less than 1.3% compared with element (1,1)] and the non-diagonal elements are zero.

We demonstrate the QST by transferring ρ_0 from spins

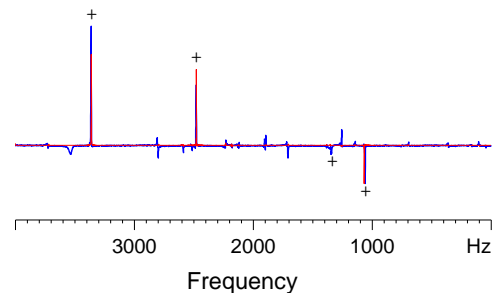


FIG. 3: (Color online) NMR spectra for implementing the selective excitation and quantum data bus for spin 2.

1 to 4 by choosing $\rho_0 = \sigma_x, \sigma_y, \sigma_z$ and I , respectively. We firstly prepare $|000\rangle\langle 000|\rho_+ - |111\rangle\langle 111|\rho_-$ by applying $R_y^4 = e^{-i\pi\sigma_y^4/4}$ to ρ_{ini} , where $\rho_{\pm} = |\pm\rangle\langle \pm|$ with $|\pm\rangle = (|0\rangle \pm |1\rangle)/\sqrt{2}$. The experimental result is shown in Figure 2 (a). The NMR peaks marked by "+" indicate the single-quantum transitions in $|000\rangle\langle 000|\rho_+$ and act as the target signals for the following QST (up to an overall phase). Because $T_{j,n}$ is spin-preserving, such transitions can represent the QST starting with the input state $\rho_0|000\rangle\langle 000|$. We therefore can ignore $|1111\rangle\langle 1111|$ in ρ_{ini} and omit the spectra in minus frequency part.

The input state is prepared by applying an operation U_{ini} to ρ_{ini} . With increasing n , $T_{1,n}$ transforms $\rho_0|000\rangle\langle 000|$ to $|000\rangle\langle 000|\rho$ asymptotically, where $\rho = e^{in\theta\sigma_z/2}\rho_0 e^{-in\theta\sigma_z/2}$. In experiments we removed the phase factor between ρ and ρ_0 by phase correction. For a fixed n , we implement the unitary $T_{1,n}U_{ini}$ using one GRAPE pulse. The experimental results of the QST after 100 iterations for the various input states are shown as Figures 2(b-e), respectively. The weak signals in figure (e) confirm the correct transfer of I .

Exploiting the transformation between the computational basis and energy eigenbasis, and ignoring the difference of T_2^* of the four protons, we can approximately obtain $A_{k,n}$ [see Eq. (5)] in the output states through measuring the amplitudes of the peaks marked by "+" in Figures 2(a-d). Therefore we obtain $p_n = |A_{4,n}|^2$. For the input states $\sigma_x|000\rangle\langle 000|$, $\sigma_y|000\rangle\langle 000|$, $\sigma_z|000\rangle\langle 000|$, p_{100} is measured as 0.97, 0.94 and 0.95, respectively. All other $|A_{k,100}|^2$ are below 0.05. To observe p_n increasing with n , we also implement the QST by choosing various n when the input state is $\sigma_x|000\rangle\langle 000|$. The measured p_n is shown as the data marked by "x" in Figure 1 (a).

We implement the selective excitation / quantum data bus for spin 2. The reverse QST starts with the input state $|000\rangle\langle 000|\sigma_x$ obtained by applying $R_y^4 = e^{-i\sigma_y^4\pi/4}$ to ρ_{ini} . When $n = 100$, $T_{2,n}^{-1}$ transforms $|000\rangle\langle 000|\sigma_x$ to $|0\rangle\langle 0|\rho|00\rangle\langle 00|$ with probability close to 1, where $\rho = e^{-in\theta\sigma_z/2}\sigma_x e^{in\theta\sigma_z/2}$. The experimental results are shown as Figure 3. The fidelity of excitation is measured as 0.98.

We choose $|\psi_{14}\rangle = (|1\rangle + |4\rangle)/\sqrt{2}$ as the target to demonstrate the generation of entanglement in spins 1

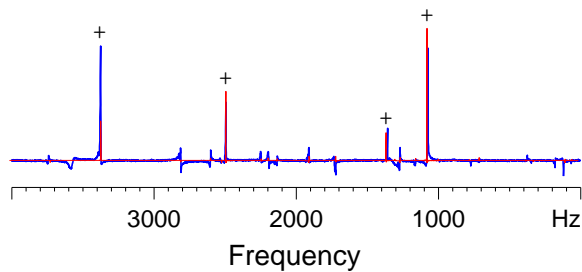


FIG. 4: (Color online) NMR spectra for measuring the fidelity of the generation of $(|1\rangle + |4\rangle)/\sqrt{2}$.

and 4. To measure the fidelity, we rewrite Eq. (8) as $p_n = |\langle 0000 | \Psi_n \rangle|^2$ [16]. Here $|\Psi_n\rangle = P^\dagger T_{1,4,n}^{-1} |4\rangle$ where P denotes the operation to prepare $|\psi_{14}\rangle$ from $|0000\rangle$ (e.g. see [17]). When p_n is close to 1, we can obtain p_n approximately by applying a readout operation $e^{i\pi\sigma_y^1/4}$ to $|\Psi_n\rangle$. Noting that $|1111\rangle\langle 1111|$ in ρ_{ini} does not contribute observable signals for measuring p_n , we approximate p_n as the coherence

$$C_n = \text{Tr}(2|0000\rangle\langle 1000|\rho_n) \quad (10)$$

where $\rho_n = U_{tot,n}\rho_{ini}U_{tot,n}^\dagger$ with $U_{tot,n} = e^{i\pi\sigma_y^1/4}P^\dagger T_{1,4,n}^{-1}e^{i\pi\sigma_x^4/2}$. The numerical simulation for C_n is shown in Figure 1 (b). One finds that C_n approximates p_n well when $n > 2$.

In the experiment we can obtain C_n up to a constant factor through measuring the single transitions in ρ_n ,

noting that $P^\dagger T_{1,4,n}^{-1}$ is not spin-preserving. Actually such a factor is not relevant if we only concern the increase of C_n with iterations. The measured C_n is shown in Figure 1 (b). Figure 4 illustrates the NMR spectra when $n = 8$.

The operations U_d , U_d^\dagger , R_y^4 , $T_{1,n}U_{ini}$, $T_{2,n}^{-1}R_y^4$, and $U_{tot,n}$ are experimentally implemented using the GRAPE pulses with fidelities larger than 0.99, respectively. The pulse lengths are 10 ms for U_d and U_d^\dagger , 20 ms for the other pulses. The experimental errors could mainly result from the inhomogeneities of the magnetic field, imperfection of GRAPE pulses and decoherence. In order to estimate the quality of the experimental spectra, we also list the ideal ones in simulation, shown as the red thin curves in Figures 2-4.

In conclusion, we have shown how various important tasks of quantum control can be achieved *indirectly* by controlling the end of a spin chain. Firstly, we implemented the transfer of an arbitrary quantum state. The dipolar couplings naturally existing in the liquid crystal NMR system are directly exploited for the QST. Our method is efficient and scalable in large size systems. Secondly, by implementing the reverse QST, we have created a full quantum data bus which is controlled by the two-qubit end gates. Finally as another application of the reverse QST, we proposed and demonstrated new methods to generate entanglement.

We thank D. Cory, C. Ramanathan, S. Bose, G. B. Furman and T. S. Mahesh for helpful discussions. DB acknowledges support by the EPSRC grant EP/F043678/1.

-
- [1] S. Bose, Phys. Rev. Lett. **91**, 207901 (2003).
[2] S. Bose, Contemporary Physics **48**, 13 (2007); D. Burgarth, arXiv: 0704.1309 [quant-ph].
[3] M. Christandl et al., Phys. Rev. Lett. **92**, 187902(2004).
[4] C. D. Franco, M. Paternostro, M. S. Kim, Phys. Rev. Lett. **101**, 230502 (2008).
[5] E. B. Fel'dman and A. I. Zenchuk, arXiv:0809.1967v1 [quant-ph].
[6] P. Cappellaro, C. Ramanathan, and D. G. Cory, Phys. Rev. Lett. **99**, 250506 (2007).
[7] D. Burgarth, V. Giovannetti, S. Bose, Phys. Rev. A **75**, 062327 (2007).
[8] J. Zhang et al., Phys. Rev. A **76**, 012317 (2007).
[9] J. Fitzsimons and J. Twamley, Phys. Rev. Lett. **97**, 090502 (2006); J. Fitzsimons et al., Phys. Rev. Lett. **99**, 030501 (2007); P. Cappellaro, C. Ramanathan, and D. G. Cory, Phys. Rev. A **76**, 032317 (2007).
[10] In our experimental system, we directly implemented the backward time evolution $U_{-\tau}$ of $Q_{j,n}^{-1}$ by forward evolution of $-H$. This is not necessary [2] but simplified the presentation. Actually one can design $Q_{j,n}$ in the Eq. (4) for the reverse QST using $-H$. Hence in the implementation of $Q_{j,n}^{-1}$ the evolution is still U_τ .
[11] D. G. Cory, J. B. Miller, and A. N. Garroway, J. Magn. Reson. **90**, 205 (1990).
[12] M. K. Henry et al., Phys. Rev. Lett. **99**, 220501 (2007); T. S. Mahesh and D. Suter, Phys. Rev. A **74**, 062312 (2006).
[13] J. Baum et al., J. Chem. Phys. **83** 2015 (1985); J.-S. Lee and A. K. Khitrin, Phys. Rev. A **70**, 022330 (2004); J. Chem. Phys. **122**, 041101 (2005).
[14] G. B. Furman, J. Phys. A **39**, 15197 (2006).
[15] J. Baugh et al., Phys. in Can. **63**, No. 4 (2007), "Special issue on quantum information and quantum computing"; N. Khaneja et al., J. Magn. Reson. **172**, 296 (2005); C.A. Ryan et al., Phys. Rev. A **78**, 012328 (2008).
[16] J. Zhang et al., Phys. Rev. A **79**, 012305 (2009).
[17] I. L. Chuang et al., Proc. R. Soc. London, Ser. A **454**, 447 (1998).